

## Refraction and reflection FWI for high-resolution velocity modeling in Mississippi Canyon

Dhananjay Tiwari\*, Jian Mao, Xuening Ma TGS

### Summary

Full waveform inversion (FWI) in recent years is widely used in the Gulf of Mexico area to optimize the accuracy and resolution of the subsurface velocity model. A velocity model using tomography is heavily dependent on the signal-to-noise ratio of the migrated common image gathers (CIG). Events are well defined on the CIG under the gas pockets, which makes it difficult to derive decent quality residual moveout picks (RMO) for input to the tomography engine. Adapting a model-building approach from the image domain to the data domain in such a geological scenario can help improve the velocity model and therefore the final image quality. The presence of a salt reflection in the Gulf of Mexico (GOM) data causes a big mismatch between the observed and predicted data near the top of salt boundary due to an inaccurate salt model. Eliminating the reflection associated with the salt from the observed data can help reduce the effect of a mismatch near the salt boundary from the data residuals when starting with a sediment-only model. We present this full waveform inversion (FWI) case study in an area of the GOM where our workflow helped capture the gas anomaly in the model and to improve the sediment model by damping the effect of salt-related energy from the input to the FWI.

### Introduction

Better illumination and fold coverage is one of the advantages of wide-azimuth data. Wide-azimuth data in the GOM area is proven to optimize the velocity model and imaging. Optimization of the velocity model using tomography is heavily dependent on the quality of residual moveout picked on migrated common image gathers (CIG).

Confidence in a derived velocity model from the reflection-based tomography is high in a good signal-to-noise ratio area, but in the presence of a gas chimney, the quality of reflected energy is very poor due to poor contrast of the acoustic impedances. Also, the contrast in the velocity model is very high between the gas-charged sediment and the normal sedimentary deposits. Updating the velocity model under such a geological regime is very challenging using tomography. Extending a model-building approach from conventional tomography to the FWI can help incorporate the low-velocity anomaly associated with the gas-charged sediment into the velocity model. We minimize the differences between observed and synthetic data in terms of amplitude and phase (Lailly, 1983; Tarantila, 1984) by updating the velocity model. Each shot in the wide-azimuth data covers more area; therefore, a coarse-grid shot density can be used during the FWI

workflow to optimize the cost and quality. Interaction of reflection and refraction energy from the salt boundary with the suprasalt sediment creates a big mismatch between observed and synthetic data if the starting model is sediment. A salt model can be used as a starting model to minimize this effect to some extent. We can use the salt model as starting model for FWI and then an iterative approach of updating the salt model at every FWI update (Wang, 2015) can be used. But this approach is very expensive when using it for medium to large 3D seismic projects, especially if the target is to optimize the supersalt velocity model. Another approach to handle the mismatch near the salt is to remove or attenuate the salt-related energy from the input data. Attenuating the energy associated with the salt boundary from the acquired seismic at the beginning of the project can help reduce the mismatch between observed and synthetic data while using the sediment model. Using this approach can save several iterations of adjusting the salt interpretation during FWI iterations and thus the overall cost. We have a robust multistage FWI for high-resolution model building (Mao et al., 2016).

We present an FWI case study on 3D-WAZ data from the GOM aiming to derive the improved velocity model with the optimized workflow in terms of cost and quality.

### Survey Area and data challenges

FWI is applied to over 100 OCS blocks in Mississippi Canyon (Figure 1) selected from the 3D-Fusion project. The red polygon identifies the area for the FWI.

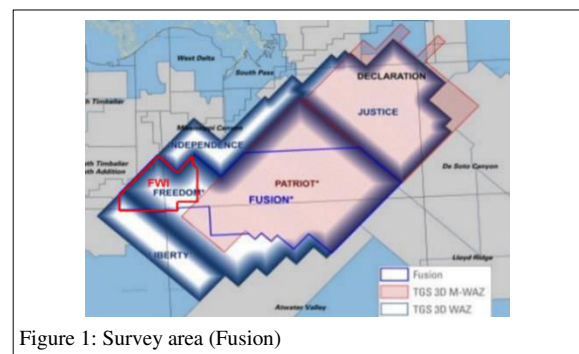


Figure 1: Survey area (Fusion)

One motivation to move forward with the FWI approach can be clearly understood from the data example shown in Figure 2. Figure 2(a) is a depth slice of seismic, corendered with the underlying velocity model prior to the FWI. The yellow-highlighted area shows the low-velocity anomaly in the velocity model. Figure 2(b) and 2(c) shows the cross-

## Refraction and Reflection FWI case study

section view along the inline and crossline within the same survey. Clearly both the inline and crossline show the underlying imaging challenges associated with the unresolved low-velocity anomaly, highlighted in the circled area.

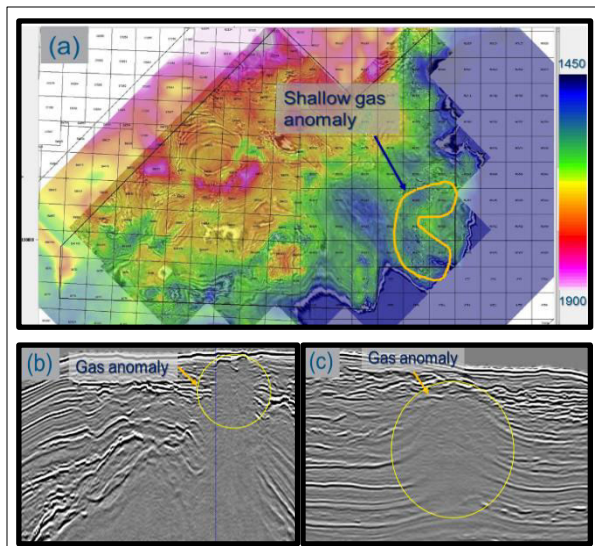


Figure 2: (a) Depth slice corendered with the underlying velocity model shows the low-velocity anomaly within the survey highlighted in yellow area (b) inline (c) crossline view of Kirchhoff depth migration stack.

Deriving the necessary velocity updates from the conventional tomography around the circled area is severely constrained by the poor S/N of the data which makes it very difficult to get decent quality RMO picks on CIGs for the tomography. In such a geological environment, FWI can benefit in updating the model in a reflection quiet zone as FWI depends on the residual of recorded and synthetic seismic data instead of RMO picks.

### FWI model updates

Updating a model from the FWI is a multistep process that can be broadly described in three steps for simplicity:

- 1) Derive a good initial velocity model (IVM) for the FWI by a conventional approach of model updating through a few iterations of tomography.
- 2) Input data preconditioning for FWI that includes the wavelet estimation and removal of the salt-related energy from the input.
- 3) Optimize the velocity model from FWI

### Initial velocity model for FWI:

A legacy anisotropic final velocity model smoothed and calibrated with the available check shot within the survey,

is used to run the prestack Kirchhoff depth migration (KDM) and first iteration of tomography. KDM gathers using an updated model from the first pass of tomography are then used in Focusing Analysis (Cai et al., 2009 and He et al., 2009) to derive the anisotropic parameters.

The multi-WAZ data are then sectorized into six azimuths to begin the azimuth-sectorized tomography. We perform two passes of TTI tomography to optimize the suprasalt velocity model. The tomography-updated model is used as a starting model for FWI.

### Input data preparation:

Wavelet estimation is the first crucial part in the FWI workflow. Synthetic data created for a line using the initial velocity model and the wavelet used to debubble of input. We select the near offset from the synthetic and the input shot, using the combination to derive the matching filter operator to match the synthetic shot to the real input data. The matching filter operator is then applied to the initial wavelet to produce a first pass of an optimized wavelet. Further coarse-grid synthetic shots are generated for the whole survey using the updated wavelet and initial velocity model. We select the near trace from the coarse grid synthetic and input shots to derive the final matching filter operator. This matching filter operator then applied to the first pass of wavelet to get the final pass of optimized wavelet.

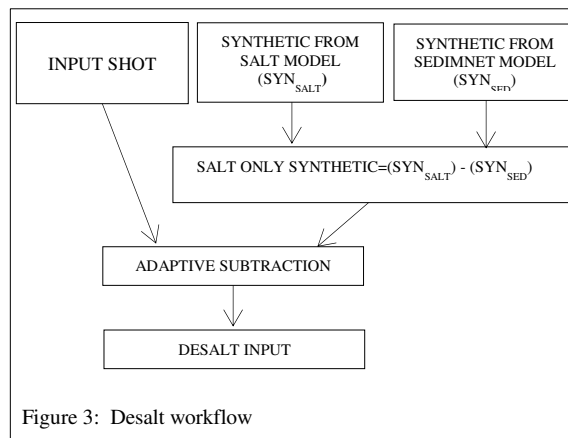


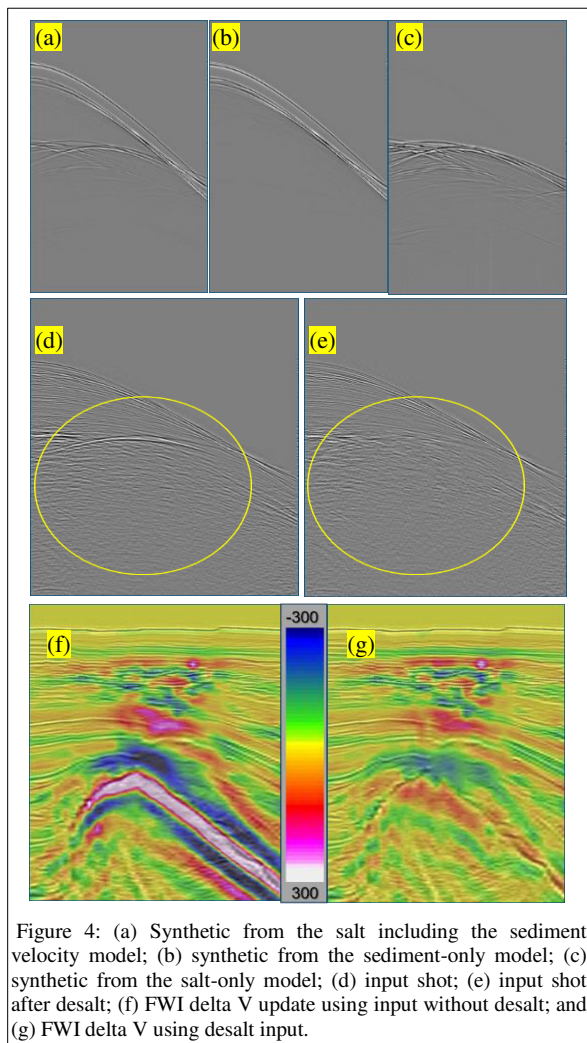
Figure 3: Desalt workflow

The interaction of reflections from the salt, create a significant mismatch between the observed and synthetic data. There are two ways to minimize the large residuals. The first is to include the salt model into the FWI and iteratively adjust the interpretation as we improve the model update from FWI.

Another method is to remove or attenuate the salt-related energy from the input data and use the sediment only model

## Refraction and Reflection FWI case study

for suprasalt FWI model updates. Starting with the salt model and continually adjusting the model involves significant salt interpretation after every update of FWI. For a large project, the cost of the FWI model increases multifold using this approach. We have adopted the second approach by attenuating the salt-related energy from the input in the beginning and using that data for all FWI iterations.



We use the salt horizons from our library to build the salt model that is used to create the synthetic. We also create a synthetic from the sediment model. Synthetic data from the salt and sediment model were subtracted to get only the reflection associated with the salt. The salt reflection is then adaptively subtracted from the input data to attenuate the salt-related energy from the input data. Figure 3 shows the desalt workflow.

Figure 4 shows an example of desalt. Figure 4(a) is the synthetic model from the salt model and Figure 4(b) is the synthetic model from the sediment-only velocity model. A direct subtraction of these two synthetics will give the energy associated with the salt boundary (Figure 4c). The salt synthetic as shown in Figure 4(c) is adaptively subtracted from the input data (Figure 4(d)). Figure 4(e) is the output after the adaptive subtraction from the salt synthetic. The salt-related energy circled in Figure 4(d) is attenuated after the adaptive subtraction as shown in Figure 4(e). To make the desalt cost effective, the highest frequency of the two synthetic models is kept close to FWI highest possible frequency. This way we only need to create the desalt input once and then it can be used for all FWI iterations starting from low frequency to high frequency. The impact of desalt on the FWI model update near the salt boundary can be seen by comparing Figure 4(f) and Figure 4(g). Clearly the large model update (delta V) near the salt is attenuated using the desalt input for FWI.

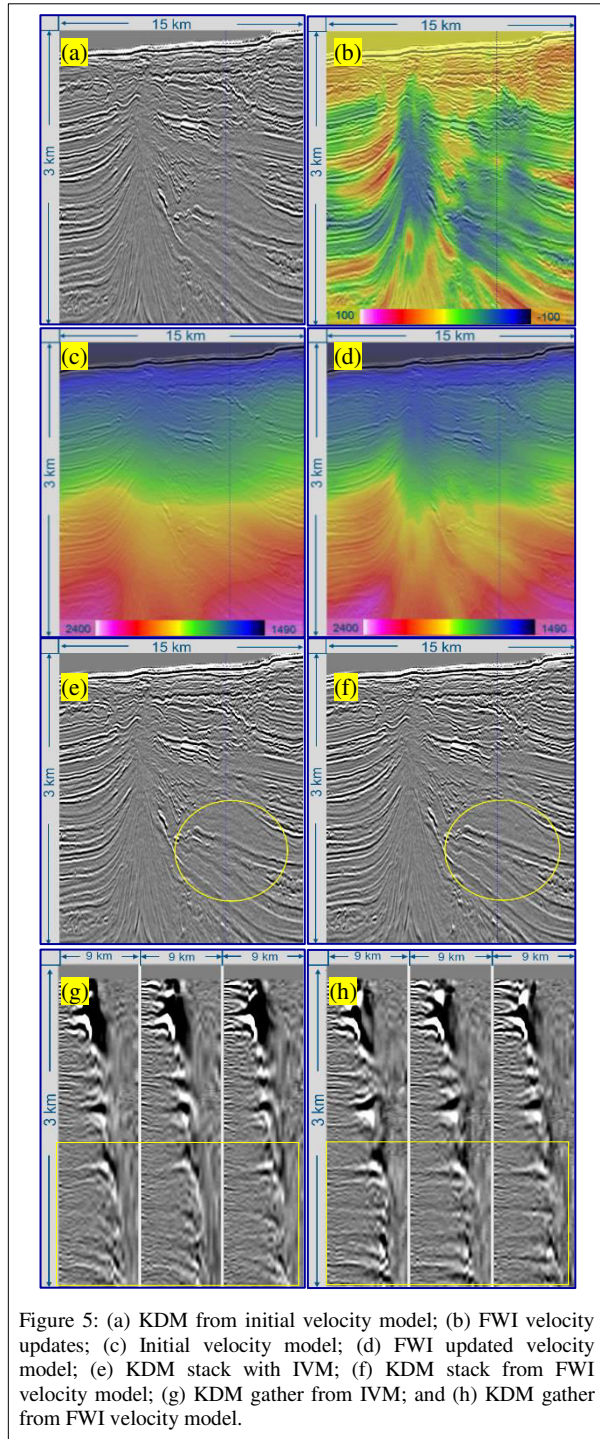
### FWI model update:

We begin with the anisotropic velocity model. Throughout the FWI we kept anisotropic ( $\epsilon$  and  $\delta$ ) fixed, updating only the velocity. Density is calculated from the velocity using Gardner's relationship (Gardner et al., 1974). An anisotropic wave equation with free-surface boundary condition is used in FWI. A ray-tracing profile is analyzed to understand the maximum depth and offset range for a diving wave FWI. Based on the maximum penetration depth from the ray tracing we interpret key horizons on a migrated stack, which are then converted to time and updated to the desalt input shot gather as a mute function during FWI. The mute is applied to the shot gather to keep only the early arrivals for the diving wave FWI. Three frequency bands starting from 3 Hz up to 12 Hz are selected for FWI. A total of five iterations for each frequency band is applied to update velocity from the diving wave FWI. Image-guided smoothing is applied to the gradient to minimize the footprint and swing noise but at the same time retain the high-frequency details derived by the FWI. The diving wave FWI update model is used as a starting model for reflection FWI (RFWI). RFWI is also applied to the three frequency bands with five iterations for each frequency band. We update density after each iteration of FWI to minimize the density leakage to the RFWI velocity model updates.

### FWI Results

Figure 5 shows the refraction and reflection combined FWI results. Figure 5(a) is the inline cross section; the amplitude shadow zone indicates the possibility of low-velocity gas-charged sediment.

## Refraction and Reflection FWI case study



We anticipate a negative velocity update ( $\Delta V$ ) from the FWI surrounding the amplitude shadow zone. Figure 5(b) shows the FWI velocity updates, corendered on the seismic to highlight the  $\Delta V$  relation to the seismic. We can see the negative velocity updates derived from the FWI surrounding the amplitude shadow zone. Another point to notice on Figure 5(b) is that the derived FWI model update trend does follow nicely with the underlying seismic image as we apply the image-guided smoothing on the gradient during FWI. Image guided smoothing of gradient field leads to the geologically constrained model updates. Figure 5(e) and 5(f) are the KDM stack from the IVM and the FWI velocity model respectively. The FWI model helps to improve the continuity of the image highlighted in the circled area. Figure 5(g) and 5(h) are gather comparisons from the KDM between initial velocity model and FWI velocity model. The initial velocity model has already gone through one iteration of high-resolution shallow tomography and two iterations of suprasalt tomography to update the velocity model. We can still see a lack of adequate resolution in the model, which may have caused over and under moveout correction of the KDM gather under the highlighted yellow rectangular box [Figure 5(g)]. The KDM gather using the FWI did bring the required resolution in the model to help flatten the KDM gather in the highlighted area [Figure 5(h)] that resulted in the improved continuity of the image [Figure 5(f)].

### Conclusions

We update the velocity model through the FWI on a recent project. We have successfully shown the impact of adapting a desalt workflow on the FWI results. Removing or attenuating salt-related energy from the input data helps reduce the high velocity updates near the salt. Image-guided smoothing during the FWI is applied to perform smoothing constrained by the seismic to retain the high-resolution feature updates from the FWI. Diving-wave FWI produces the low-frequency background velocity updates to the models. Several iterations of reflection FWI in addition to the diving wave FWI allow us to further fine tune the velocity model in terms of capturing some high-resolution velocity anomalies like gas channels. KDM stack and gather both have shown the improvement using the final FWI model velocity model over the initial velocity model.

### Acknowledgments

Authors would like to thank Zhiming Li, Bin Wang and James Sheng for their contribution. We also thank Connie VanSchuyver for reviewing the manuscript and the management of TGS and WesternGeco JV for permission to publish this paper

## REFERENCES

- Cai, J., Y. He, Z. Li, B. Wang, and M. Guo, 2009, TTI/VTI anisotropy parameters estimation by focusing analysis, Part I: Theory: 79th Annual International Meeting, SEG, Expanded Abstracts, 301–305, <https://doi.org/10.1190/1.3255480>.
- Gardner, G., and L. W. Gardner, and A. R. Gregory, 1974, Formation velocity and density—The diagnostic basics for stratigraphic traps: *Geophysics*, **39**, 770–780, <https://doi.org/10.1190/1.1440465>.
- Lailly, P., 1983, The seismic inverse problem as a sequence of before stack migrations: Conference on Inverse Scattering, Theory and Application, Society of Industrial and Applied Mathematics, Expanded Abstracts, 206–220.
- Mao, J., J. Sheng, M. Hart, and T. Kim, 2016, High-resolution model building with multistage full-waveform inversion for narrow-azimuth acquisition data: *The Leading Edge*, **35**, 1031–1036, <https://doi.org/10.1190/tle35121031.1>.
- Tarantola, A., 1984, Inversion of seismic reflection data in the acoustic approximation: *Geophysics*, **49**, 1259–1266, <https://doi.org/10.1190/1.1441754>.
- Wang, K., B. Deng, Z. Zhigang, and H. Lingli, 2015, Top of salt impact on full waveform inversion sediment velocity update: 85th Annual International Meeting, SEG, Expanded Abstracts, 1064–1069, <https://doi.org/10.1190/segam2015-5878985.1>.